



EXPERIMENTAL AND NUMERICAL INVESTIGATIONS ON THE STRUCTURAL RESPONSE OF PRECAST CONCRETE UNDERPASSES SUBJECTED TO LIVE LOADS

Fernando António Baptista Branco^{1✉}, Mário Rui Tiago Arruda²,
João Pedro Ramôa Ribeiro Correia³

Dept of Civil Engineering and Architecture, Instituto Superior Técnico / ICIST,
Technical University of Lisbon, Av. Rovisco Pais 1, 1049-001 Lisboa, Portugal
E-mails: ¹fbranco@civil.ist.utl.pt; ²marruda@civil.ist.utl.pt; ³jcorreia@civil.ist.utl.pt

Abstract. This paper presents results of experimental and numerical investigations on the structural response of precast concrete underpasses when subjected to the effects of vehicular live loads. *In situ* full-scale load tests were carried out on three different precast concrete underpasses, with inner radii of 6.50 m, 3.00 m and 1.50 m. In these tests, the structural response of the underpasses when subjected to load trucks was assessed in terms of their radial deflections. Numerical investigations included the development of linear elastic 2D and 3D finite element models of the underpasses tested. Based on the good agreement between experimental data and numerical calculations, load distribution factors were computed for different forces (bending moments, compression and shear) and these can be used for design purposes. The paper analyses also the effects of varying the thickness of the cover soil and the thickness of the concrete arch in the load distribution factors of precast concrete underpasses.

Keywords: underpass, precast concrete, live loads, experimental tests, numerical models, finite element models, load distribution factors.

1. Introduction

In the last two decades, with the considerable expansion of several highway networks, there has been an increasing use of precast concrete arch underpasses due to the advantages they offer over traditional solutions (cast *in situ*), namely in terms of speed and ease of erection, quality control (materials and geometry) and economy. In addition, what regards their structural response, the existence of radial dry joints (that in general comprise partial hinges) allows reducing the overall bending stiffness of the structure, thereby reducing the maximum stress values compared to equivalent monolithic frame systems.

Precast concrete arch underpasses are basically made of several individual modules (most often, semi-circular) that are assembled on site, constituting a buried tunnel structure that is subsequently covered with layers of soil and the road pavement (often built according to the *cut-and-cover* tunnelling technique). These structures may also include lower horizontal elements closing the cross-section at the footing level.

This type of structures is mainly subjected to the effects of the cover soil and those of vehicular loads. The live loads are especially difficult to simulate as they are associated with

a complex soil-structure response. Typically, when a truck approaches these arches, the first half of the structure first presents inwards radial deflections, while the second half of the structure deflects outwards in the radial direction. Subsequently, when the truck moves away and passes the top of the arch, those signs are inverted. The forces that develop in the concrete structure during this movement are significantly influenced by the soil-structure interaction.

The design of concrete underpasses is currently performed with simplified two-dimensional (2D) finite element (FE) elastic models or even with plane frame models, in which the soil-structure behaviour and the effect of live loads is difficult to be accurately evaluated. Nevertheless, the correct quantification of the effects of live loads is essential, especially in underpasses with a thin layer of cover soil (min recommended value is typically around 0.60 m), in which live loads cause higher forces in the structure.

Presently, the considerable reduction of computational costs enabled the development of sophisticated numerical three-dimensional (3D) models, taking into account the construction phases and the soil-structure interaction. For common arch bridges, such developments are already well-established (Au *et al.* 2003; Zanardo *et al.* 2004). Several studies have also been already reported for masonry

arch bridges (Boothby *et al.* 1998; Fanning *et al.* 2001; Fanning, Boothby 2001) and box-culvert concrete underpasses (Chen *et al.* 2010; Pimentel *et al.* 2009). What concerns the particular case of precast concrete arch underpasses, much less results are available in the literature; with this regard, it is worth mentioning the work reported by Zoghi and Farhey (2006) on the assessment of construction and live loads on buried small arch bridges, and also the study presented by Audenaert *et al.* (2008) on the prediction of the resistance of this kind of structures. However, the numerical work developed by these authors comprised only 2D models and only results presented by Zoghi and Farhey (2006) were validated with experimental tests.

This paper presents results of experimental and numerical investigations on the behaviour of precast concrete underpasses under the effects of live loads, allowing understand in much further depth their structural response. Three types of underpasses were studied, with different geometries and structural systems. The experimental programme included full-scale *in situ* tests on the three underpasses and provided the influence lines of radial deflections. The numerical study included the development of 3D models of the underpasses studied, which were validated based on results of load tests. These models were used:

- to compute load distribution factors applicable in engineering practice which are still not available in the technical literature;

- to study the effects of varying the thickness of the concrete arch and that of the cover soil, an aspect that has been reported earlier for box-culverts (Chen *et al.* 2010), but not for precast concrete arch underpasses;
- to evaluate the effects of loads defined in different regulations, namely *EN 1991-2: 2003 Eurocode 1: Actions on Structures – Part 2: Traffic Loads on Bridges* (EC1) and the *Portuguese Code for the Safety of Buildings and Bridges* (RSA).

2. Characteristics of the precast underpasses

This chapter describes the geometry, materials and construction of the three different types of precast concrete underpasses studied, referred to as PA1, PA2 and PA3, and shown in Fig. 1. The underpasses were developed by company *Pavicentro, Portugal*, and are being used under highways as road underpasses, and also as agricultural or hydraulic underpasses.

Fig. 2 illustrates the cross-section of the three types of underpasses. In the longitudinal direction, they are all composed of several precast concrete modules each with a length of 1.50 m. In underpass PA1 modules are made of concrete type C30/37, according to *EN206-1: 2000 Concrete – Part 1: Specification, Performance, Production and Conformity*, while in underpasses PA2 and PA3 they are made of concrete type C25/30.

PA1 (under construction)

PA2

PA3



Fig. 1. Views of the three types of underpasses studied

PA1

PA2

PA3

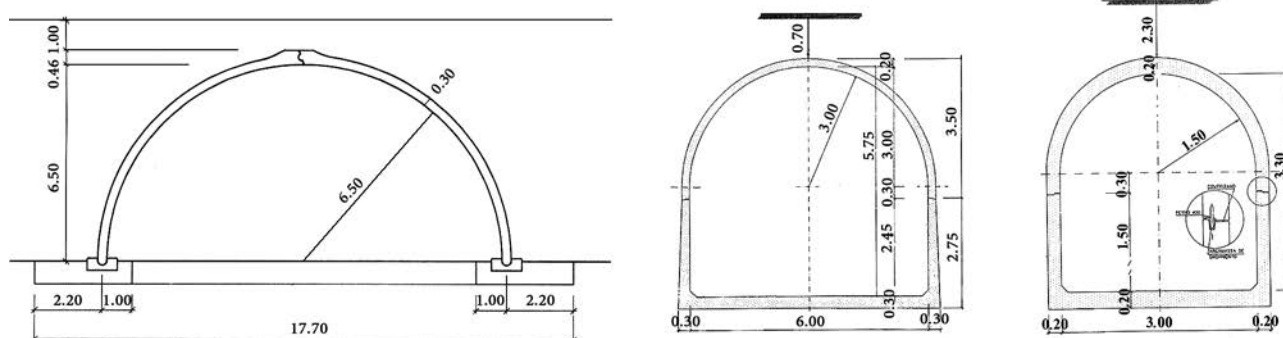


Fig. 2. Cross-section of the three types of underpasses studied (dimensions in m)

Underpass PA1 corresponds to a circular arch with an inner radius of 6.50 m and a thickness of 0.30 m. The bases of the arch are founded in 3.10 m wide \times 0.70 m high footings, being placed on top of 1.00 m wide precast elements. The connections between the precast modules and the footings and the connections between the modules at the top of the arch are all hinged – these latter connections present a curved connector that interconnects the two opposite elements. In the longitudinal direction the modules are placed in an alternate configuration (i.e. the centre of a module on one side is aligned with the lateral edge of a module on the opposite side). After placing the modules, longitudinal prestress cables are positioned at the top and bottom of the arch in order to assemble the individual modules. The prototype underpass tested presents 5 modules on one side and 6 on the other, corresponding to total lengths of 7.50 m and 9.00 m, respectively. The cover soil is approx 1.00 m thick (measured at the top of the arch relatively to its top face, after mechanical compaction), including mostly homogeneous sandy terrain and, in a lesser extent, sandy terrain with some mixture of organic soil. Prior to the load test, a thin layer of gravel was laid on the top of the cover soil to facilitate the circulation of the load truck.

Underpass PA2 is composed of semi-circular upper elements, with an inner radius of 3.00 m, supported on U-shaped elements with a height of 2.75 m (measured from the bottom face of its platform base). The slab thickness varies between 0.20 m (in the arch) and 0.30 m (in the platform base). The connection between the semi-circular upper elements and the U-shaped bottom elements is provided by $\varnothing 20$ mm steel connectors, filled with cementations grout. The cover soil is approx 0.70 m thick,

including the bituminous pavement of the highway that crosses the underpass.

Underpass PA3 presents a similar geometry to that of underpass PA2 but is made of smaller elements. The inner radius of the semi-circular upper elements is 1.50 m and the height of the U-shaped elements is 1.70 m. All underpass modules present a thickness of 0.20 m. The connection between the semi-circular upper elements and the U-shaped bottom elements is similar to that of underpass PA2. The cover soil is approx 2.30 m thick and, as for underpass PA2, it includes the bituminous pavement of the highway crossing the underpass.

3. Experimental tests

3.1. Objectives and general methodology

The experimental tests had the following main objectives:

- to evaluate and characterize the structural behaviour of the underpasses under live loads, as they had been recently developed;
- to use the experimental data to assess the accuracy of current methods available for their design.

As referred in the introduction section, little information is available on the literature concerning the validation of current design methods with full scale load tests for this type of structures, particularly taking into account the doubts about the actual effects of the soil-structure interaction.

3.2. Instrumentation

The deflections of the underpasses when subjected to the applied loads (described in section 3.3.) were measured at different positions of their intermediate section with displacement transducers of TML brand (with a stroke of 25 mm and a precision of 0.01 mm). Transducers (9 in underpass PA1 and 7 in PA2 and PA3) were positioned in a radial configuration with respect to the instrumented cross-section, with their piston aligned perpendicularly to the lower surface of the arch. Transducers were supported in scaffolding metallic structures (independent from the underpasses). Fig. 3a illustrates the position and nomenclature of the transducers used in underpass PA1, as well as a detail of the metallic structure and one of the

Table 1. Angular position (θ in degrees, c.f. Fig. 3) of transducers used in all underpasses

Underpass	D1	D2	D3	D4	D5	D6	D7	D8	D9
PA1	17	34	55	68	90	106	125	144	159
PA2	0	27	57	90	121	149	180	–	–
PA3	0	35	73	90	109	149	180	–	–



Fig. 3. Load test of underpass PA1: a – general view and nomenclature of transducers; b – test in progress

transducers used. Table 1 lists the angular position of the transducers used in all underpasses. Data acquisition was performed using a *datalogger* from HBM – in underpass PA1 deflections were registered in a discrete mode, while in underpasses PA2 and PA3 a continuous register was made.

3.3. Applied loads and test procedure

The loads used in the tests consisted of trucks filled with sand. Underpass PA1 was loaded with a single truck (owing to its reduced width), while underpasses PA2 and PA3 were loaded with two trucks. Table 2 lists the main characteristics of the trucks used in the three load tests, namely their total weight (TW), the number of axes (NA), the load per axis (LA) and the distances between axes (DA). The transverse distance between tyres was approx 2.00 m in all trucks. In the load test of underpass PA1, the truck crossed the underpass at low speed centred in the transverse direction (Fig. 3b). In the load tests of underpasses PA2 and PA3, the two load trucks moved at low speed, one behind the other, keeping a small distance between each other. In underpass PA2 one of the trucks moved forward and the other moved backwards, while in underpass PA3 both trucks moved forward. In the transverse direction, trucks moved as close as possible to the safety barrier of underpasses PA2 and PA3.

Deflections at the instrumented cross-sections were measured during the load tests (every 2.00 m in test PA1 and continuously in tests PA2 and PA3) providing the influence lines of radial deflections. In test PA1 it was not possible to monitor the complete unloading of the underpass, because the load truck got buried at the end of the underpass. In tests PA2 and PA3 the load trucks exited the influence zone of the underpasses and therefore it was possible to monitor the complete unloading of the underpasses.

3.4. Results and discussion

Fig. 4 shows the results obtained in the three load tests, namely the influence lines of radial deflections D1 to D9 of underpass PA1 and radial deflections D1 to D7 of underpasses PA2 and PA3. The origin of the horizontal axes illustrated in Fig. 4 corresponds to the base of the arch closest to the first axis of the load truck at the beginning of the load test.

From a qualitative point of view, the pattern of variation of radial deflections measured in the test of underpass PA1 agrees with the typical behaviour exhibited by this type of arch structures. In fact, when the load truck approached the underpass, measurement points at the North side (D1 to D4) first moved inwards and then moved outwards. The

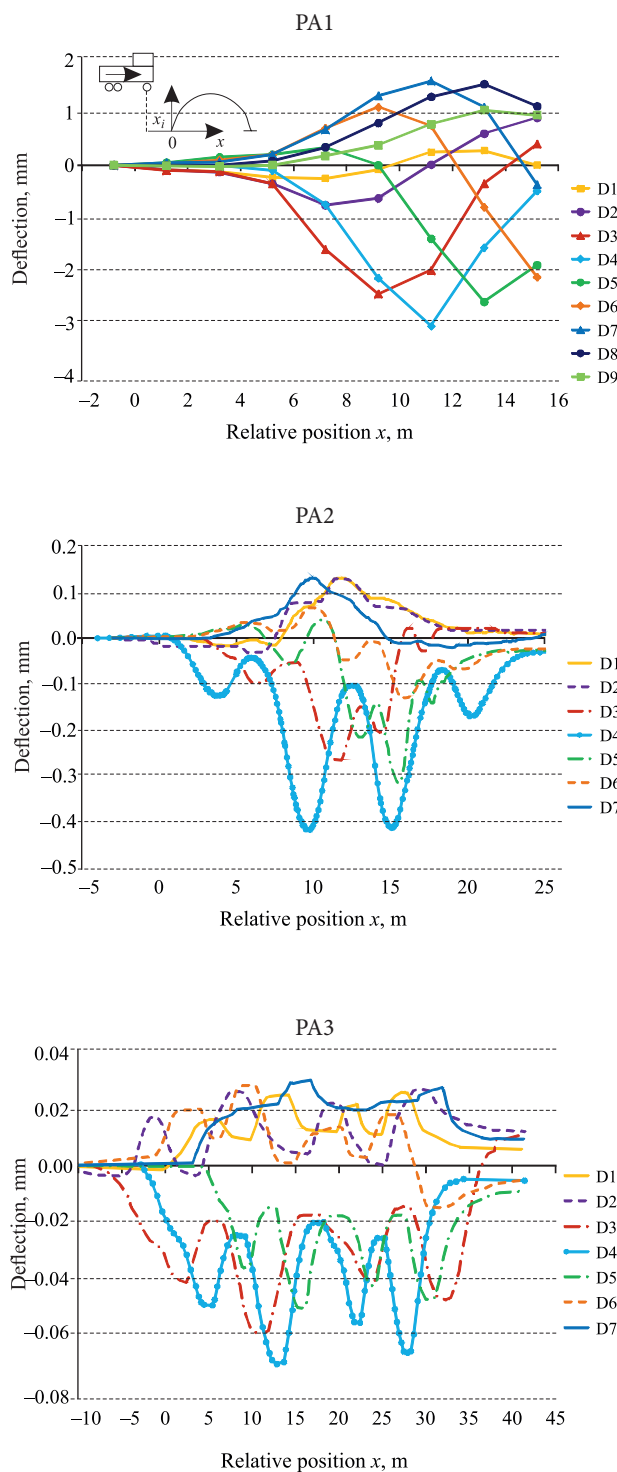


Fig. 4. Results of load tests of the three underpasses

Table 2. Characteristics of the trucks used in the load tests

Underpass	Truck	TW, kN	NA	LA, kN	DA, m
PA1	1	419	3	92.2 + 167.7 + 159.5	5.0 + 1.4
PA2	1	358	3	86 + 136 + 136	4.5 + 1.3
	2	356	3	85 + 135.5 + 135.5	5.0 + 1.3
PA3	1	428	5	91.5 + 91.5 + 81.7 + 81.7 + 81.7	3.3 + 5.7 + 1.25 + 1.25
	2	429	5	89.5 + 89.5 + 83.3 + 83.3 + 83.3	3.3 + 5.5 + 1.2 + 1.2

measurements at the South side (D6 to D9) exhibited an opposite pattern of variation, first moving outwards and then inwards. In addition, as expected, in both North and South sides, consecutive deflections present a horizontal offset. The top of the arch (D5) presented a similar pattern of variation to that exhibited by the South points, with lower upwards deflections in the first part of the test and higher inwards deflections in the second. Although it was not possible to withdraw the effect of the truck at the end of the test (as mentioned, it got buried when its rear axes were still above the underpass), measurement points at the North side presented a fairly reasonable recuperation of deflections. It is also worth mentioning the elastic response exhibited by the structure, which presented insignificant cracking levels. As expected, the max deflection at the top of the arch (2.7 mm) occurred when the back axes (the heaviest) of the load truck were aligned with the top of the arch.

Results obtained in the tests of underpasses PA2 and PA3 were qualitatively similar to those obtained in the test of underpass PA1. The continuous variation of deflections at the different measuring points of underpasses PA2 and PA3 reflects their good structural response. Those structures exhibited also an elastic behaviour, with negligible cracking and an almost full recovery of deflections after being crossed by the load trucks. In both underpasses, radial deflection curves measured by displacement transducers D4 (located at the top of the arch) presented local max values when the truck axes were aligned with the top of the arch (absolute max deflections of 0.42 mm and 0.075 mm in underpasses PA2 and PA3, respectively). The relative variation of max deflections at the top of the three underpasses (max in PA1, about 2.5 mm, and min in PA3) is due to the differences in their span and overall stiffness.

4. Numerical investigations

4.1. Description of the numerical models

The numerical investigations were carried out using commercial software SAP2000 and comprised the development of two-dimensional (2D) and three-dimensional (3D) models of all underpasses tested. The geometry of the models was identical to that of the tests. Regarding the thickness of the cover soil, two different values were used:

- the actual cover soil of the underpasses tested, referred in section 2;
- the min recommended thickness of 0.60 m.

The former value was used for the comparison with experimental results, while the latter was used to assess the

effects of design loads and to determine the values of load distribution factors. For the 2D models (Fig. 5) two types of elements were used:

- the frame element with shear deformability, to simulate the concrete arch;
- the plane element with drilling degree of freedom (two displacements and one rotation), to simulate the soil around the arch and the road bituminous layer.

For the 3D models (Fig. 5) also two types of elements were used:

- the shell element, to simulate the arch;
- the solid element with drilling degree of freedom (three displacements and three rotations), for the soil and road bituminous layer, in order to reproduce the effect of stress degradation along the height and to simulate the soil-structure interaction.

In the model of underpass PA1 the connections at the top (between modules) and bottom (to the foundation) of the arch were considered to be pinned (hinged). In the other two models (underpasses PA2 and PA3) the connections between all underpass modules (arch, lateral walls, bottom slab) were considered to be monolithic. The kinematic boundaries adopted were similar for the 2D and 3D models:

- the bottom horizontal boundary was restricted by pinned supports in all three directions;
- in order to accurately model the deformation of the soil since the beginning of the load test, the vertical boundaries only restricted the horizontal longitudinal displacements and their respective perpendicular rotations.

The total length of the model was defined as being 3 times the diameter of the arch in order to minimize the effects of the above mentioned vertical kinematic boundaries in the structural response of the arch. In all three cases the top horizontal static boundaries were defined with lanes that simulate the passage of the load trucks. To this end, line lanes and surface lanes were defined for the 2D and 3D models, respectively, with their length varying depending on the diameter of the arch.

Two types of concrete were considered in the modelling of the underpass modules, corresponding to types C25/30 with an elasticity modulus of $E_c = 31$ GPa (used in pinned arch PA1) and C30/37 with $E_c = 33$ GPa (used in continuous arches PA2 and PA3), both with a Poisson Ratio of $\nu = 0.2$. The geotechnical report refers two types of soils, namely the cover soil and the foundation soil. Based on such report, for underpass PA1, elasticity modulus of

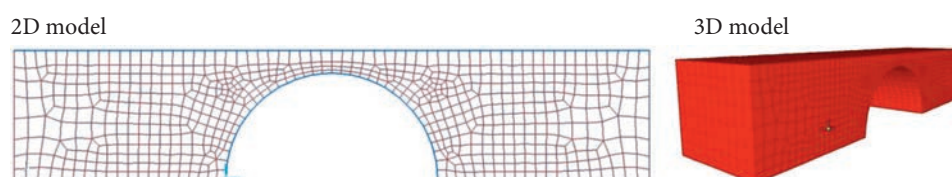


Fig. 5. Underpass PA1 – finite element meshes

$E_{s1} = 18$ MPa and $E_{s2} = 80$ MPa were adopted for the cover and foundation soils, respectively. For underpasses PA2 and PA3, in which the foundation and cover soils were more compacted, those figures were $E_{s1} = 60$ MPa and $E_{s2} = 150$ MPa. Taking into account the magnitude of the stiffness of the foundation soil when compared with that of the cover soil, it seemed reasonable to admit that the latter is completely fixed to the ground. In the models of underpasses PA2 and PA3, the road bituminous layer was also simulated, with an elasticity modulus of $E_b = 2.5$ GPa. This layer provides additional stiffness to improve the degradation of stresses due to live loads.

The loads corresponding to the trucks used in the experimental tests were simulated as concentrated loads, with the values and relative distances between axes listed in Table 2, and were positioned in their actual transverse direction (i.e. according to the load test). For comparative purposes (cf. section 4.3), two different code live loads were also considered in the models:

- those referred in EC1 that include three load trucks (each one with 2 axes distanced of 1.2 m, weighing 300, 200 and 100 kN, respectively) combined with longitudinal uniform live loads of 9 kN/m² and 2.5 kN/m²;
- those defined in RSA, that prescribes the consideration of either truck loads (with 3 axes distanced of 1.5 m, each one weighing 200 kN) or the effects of two distributed live loads – an uniform load of 4 kN/m² together with a transverse linear load of 50 kN/m.

In both EC1 and RSA, the number of trucks that need to be considered depends on the number of lanes. Due to the number of lanes located above the underpasses analysed in the present study, EC1 specifies the consideration of the first and second load trucks, while for RSA only the first truck needs to be considered for design. According to the recommendations defined in those codes, in the transverse direction, the truck loads were positioned next to the safety barriers.

Even though concrete and soil materials were involved, all analyses were linear elastic. Such modelling option was considered to be a valid approximation due to the fact that the magnitude of the loads was not high enough to produce yield behaviour on those materials. Some problems may arise in the vicinity of model singularities, but their effects are considered to be negligible for the global response of the structures. With this respect, it is worth mentioning that during the load tests, no cracks were observed in none of the underpasses when loaded by the trucks. For the lane loads, multistep static analyses were performed in which the axial loads were successively positioned in steps of 0.50 m.

4.2. Results and comparison with experimental data

In this section, results of numerical calculations are compared with experimental results in order to assess the accuracy of the 3D models developed, by comparing their outputs with real values measured *in situ* during the load tests. It is worth referring that the deflections measured during the experimental tests corresponded only to the

effects of the load trucks, because the deformations due to the self weight of the underpasses and the cover soil were already installed before the beginning of the tests. Therefore, in order to allow for reliable comparisons, numerical deflections account only for the effects of live loads.

Fig. 6 compares the experimental and numerical values (from 3D models) of radial deflections at the top of the three underpasses tested.

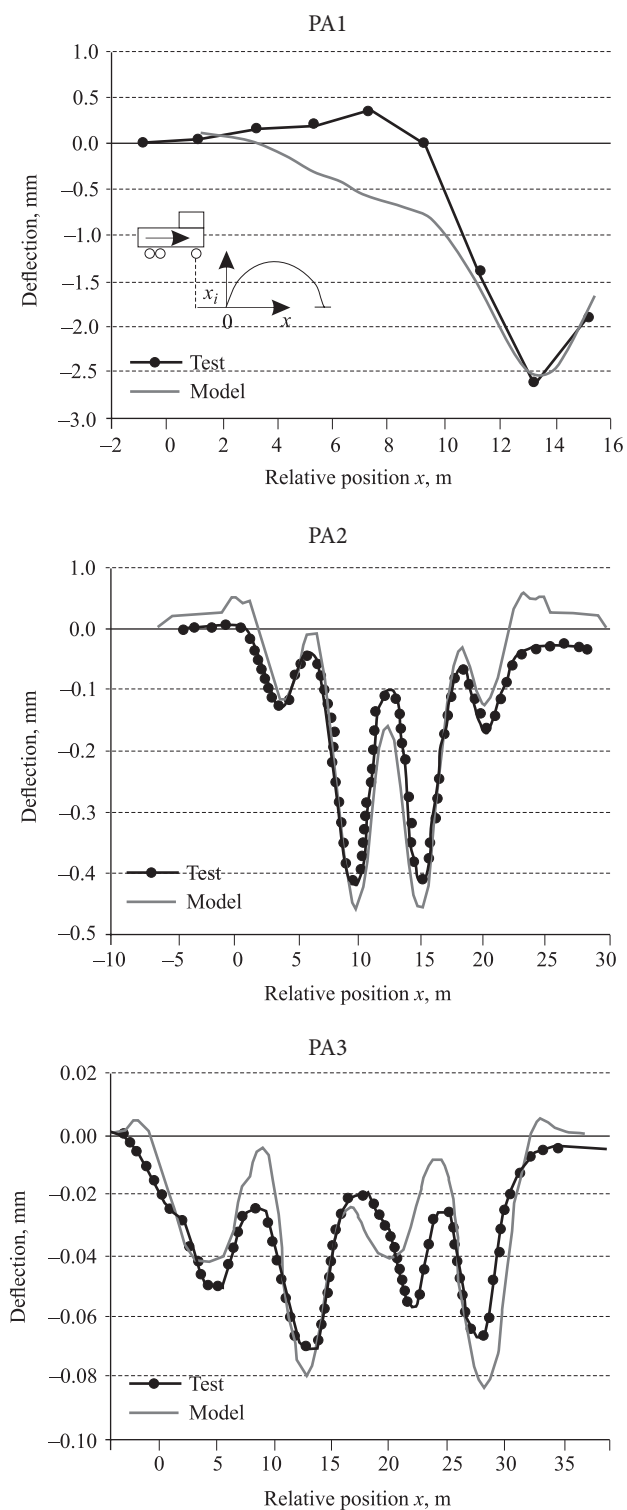


Fig. 6. Comparison of experimental and numerical radial deflections at the top of the three underpasses

Results presented in Fig. 6 show that in spite of some differences (discussed next in further detail), there is a generally good agreement between experimental curves and their numerical counterparts, particularly in what concerns the values of max deflections at the top of the underpasses. In fact, the relative differences between max deflections were 0.38%, 12.77% and 26.39% for underpasses PA1, PA2 and PA3, respectively. It is worth mentioning that the highest relative differences between experimental and numerical deflections, found in underpass PA3, correspond to very low absolute differences in deflections (less than 0.02 mm).

Differences between experimental and numerical results may stem from the following possible causes:

- differences between the actual elastic parameters of the soil and those used in the models (the typical variation of the soil's Young's modulus along the depth was not modelled);
- material non-linearities may develop in the soil due to the self weight - since the load history is not accounted for, these effects are not considered here;
- the parameters of the soil and the concrete suffer from stochastic effects since they are not deterministic (yet, as already mentioned, one expects the reinforced concrete to remain within its elastic domain, as no cracks were observed during the load tests);
- the offset between numerical and experimental peaks may have also been influenced by the difficulty in guaranteeing the predefined constant speed of the load trucks and also the distance between them (in the tests of underpasses PA2 and PA3).

In what concerns underpass PA1, in the beginning of the analysis, numerical and experimental data are very similar, but after load step 1.2 m results tend to diverge presenting a max difference of about 1 mm. From load step 11.2 m until the end of the test (as already mentioned, radial deflections were only measured until a distance of about 15.2 m from the reference axis), during which max deflections were measured at the top of the arch, experimental and numerical results converge again and are in very good agreement.

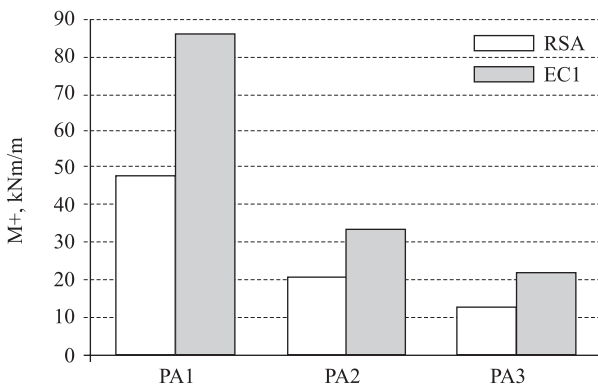


Fig. 7. Magnitude of maximum positive bending moments (M^+) for RSA and EC1 standard loads

For underpass PA2, the variations of experimental and numerical vertical deflections at the top of the arch are very similar and, furthermore, the peak values exhibited by those curves are almost identical. The highest relative difference between experimental and numerical results corresponds to the min peak values in load step 5.8 m.

Regarding underpass PA3, the agreement between experimental data and numerical calculations, although not as good as that obtained for the two previous underpasses, is still quite reasonable. In fact, not only the locations of the max and min peak values coincide, but also the magnitudes of the experimental and numerical vertical displacements present small differences.

The generally good agreement between experimental and numerical results, particularly if taking into account the non-linearity and randomness of the soil, allowed validating the models developed within the present study. Based on such validation, the next sections of this paper will address the assessment of the effects of design loads on the underpasses and, subsequently, the determination of load distribution factors to be used in design.

4.3. Assessment of the effects of design loads

This section presents a comparison of the effects of the loads defined in the RSA and those defined in EC1 in the three underpasses studied.

Load values specified in those codes suggest *a priori* that the magnitude of the effects due to EC1 loads would be higher than those due to RSA loads. As already mentioned, taking into consideration the transversal width of the circulation lanes of the three underpasses, for RSA only one load truck needs to be considered, while for EC1 two load trucks are considered.

Fig. 7 illustrates the comparison between the maximum positive bending moments (M^+) in the three types of underpasses caused by the two code loads. Results obtained in the present study clearly confirm the much higher magnitude of forces associated with EC1 design loads. In fact, for all three underpasses, the positive bending moments for EC1 design loads are almost twice than those due to RSA design loads.

Results obtained in the present study point out the fact that EC1 loads are much more conservative than those defined in RSA, for which most Portuguese bridges were designed for in recent years. Therefore, according to EC1 standard, regardless of their deterioration (Kamaitis 2012), the safety level of most of the existing precast concrete underpasses is insufficient and therefore retrofitting may be needed.

4.4. Determination of load distribution factors

For common deck girders, the load distribution factors for point loads (percentage of max bending moment per girder) are tabulated in well-known abacuses (Cusens, Pama 1975; Hambly 1976). However, those abacuses are only valid for certain types of bridge decks and are generally used to estimate the magnitude of longitudinal stresses,

when using computer AID design. For underpass arches, these abacuses are not applicable due to the following reasons:

- they are only valid for straight bridge decks;
- they only take into account the existence of load distribution factors for bending moments, providing no information about the load distribution factors for shear and axial forces, which are also very important in arch bridges;
- it is not possible to calculate distribution factors for decks with pinned connections;
- they do not consider the influence of the cover soil.

This part of the paper presents a study about the magnitude of load distribution factors for arch underpasses when subjected to the design loads defined in EC1 and analysed as plane frames. In this study the load distribution factors correspond to the ratio between the max force (moment, or axial force or shear) per unit of transverse and the corresponding total force in the cross-section. The three types of arches corresponding to underpasses PA1, PA2 and PA3 were studied, the first one comprising a pinned arch with a diameter of 13.30 m and the last two being monolithic arches with diameters of 3.00 m and 1.50 m, respectively. A cover soil of 0.60 m was considered, as it corresponds to the most conservative design situation. For underpass PA1, three critical cross-sections were considered: the max shear and min compression were determined at the bottom and top of the arch, respectively, while a section located at angle of approx 45° from the base of the arch was used to assess the max bending moments. For underpasses PA2 and PA3 (monolithic arch), only two critical cross-sections were considered: min and max bending moments were evaluated in sections at the bottom and top of the arch, respectively, while in both sections max/min shear and min compression were analysed.

Four different load cases were considered, corresponding to one (1LV), two (2LV) and three (3LV) lateral trucks positioned as close as possible to the safety rail, and one centred truck (1CV). For the lateral trucks, the load distribution factors were gathered only at the end of the transversal section, since it is there that higher stresses develop. For the centred truck, the load distribution factors were computed next to the central transversal axis. In what concerns max bending moments, cross-section 2 (top of the arch) is the most critical for the monolithic arch, while for the pinned arch the critical section is located at an angle of approx 45° from the base of the arch (cross-section 2). For min bending moments, as expected, the critical cross-section in the monolithic arch is cross-section 1. The critical section for axial compression loads is section 1 for both the monolithic and pinned arch. In what concerns shear, for the pinned arch, cross-sections 2 and 3 are critical, while for the monolithic arch cross-section 2 presents the highest forces. Fig. 8 plots the load distribution factors (LDF) obtained from the analyses carried out, namely in terms of positive (M^+) and negative (M^-) bending moments, axial compression (N^-), and positive (V^+) and negative (V^-) shear forces.

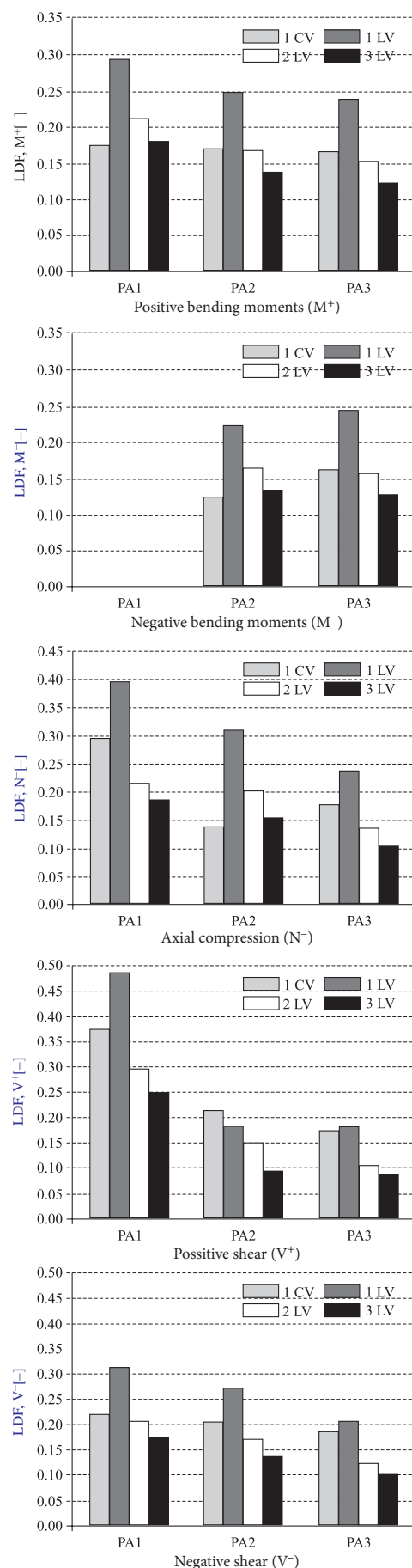


Fig. 8. Maximum load distribution factors

Results presented in Fig. 8 show that for the three underpasses studied the max values of the load distribution factors for M^+ and M^- vary between 0.25 and 0.30. It is worth noting that for deck girders the max values of the load distribution factors (provided only for M^+) vary typically between 0.60 and 0.85, depending on the bending/torsion stiffness and transverse spacing of the longitudinal beams (Cusens, Pama 1975; Hambly 1976). Such difference stems basically from the cover soil of the underpasses and the additional axial stiffness of the arches. For N^- and V^+/V^- the magnitude of the load distribution factors is higher than that for M^+/M^- , with max values varying between 0.25–0.40 (compression) and 0.20–0.45 (shear).

Results plotted in Fig. 8 show also that, in general, for all types of forces analysed the load distribution factors are higher for more flexible arches. In fact, load distribution factors in bending for underpass PA1 are higher than those for underpass PA2, which in turn are higher than those for underpass PA3 (except for M^- when loaded by a single truck). For axial and shear forces, the variation of the load distribution factors within the three different types of underpasses is also consistent with their relative stiffness, with the highest values being obtained for underpass PA1 and the lowest for PA3.

Fig. 8 also illustrates the effect of the number of load trucks and their lateral position in the load distribution

factors. As expected, load distribution factors corresponding to one lateral truck are considerably higher than those for one centred truck (in some cases, almost the double). As an example, for underpass PA1, the load distribution factors for M^+ corresponding to one lateral truck and one centred truck are respectively 0.29 and 0.18. Similarly, when the number of trucks increases, the corresponding load distribution factors consistently decrease and such variation is higher when the number of trucks increases from one to two than when it increases from two to three.

4.5. Parametric study

A parametric study was conducted in order to evaluate the importance of the thickness of the arch and that of the cover soil on the load distribution factors for positive bending moments. In the present study, only underpass PA2 subjected to the effects of two lateral load trucks defined in EC1 was considered. Fig. 9 illustrates the results of such parametric study.

Results obtained show that, as expected, for increasing values of arch thickness the values of the load distribution factors for M^+ tend to stabilize around 0.160 (for underpass PA2 with a cover soil thickness of 0.60 m). The existence of an asymptotic lower bound for increased arch thickness is caused by the increase of bending and axial stiffness's of the arch, which provides a smoother distribution of soil stresses in the arch. Regarding the thickness of the cover soil, although the values of the load distribution factors for M^+ showed some mesh dependency, they clearly decrease when the cover soil thickness increases, stabilizing around 0.170 (PA2). This variation, as expected, is due to the fact that for increasing thicknesses of cover soil the stresses are more smoothly distributed across the arch width.

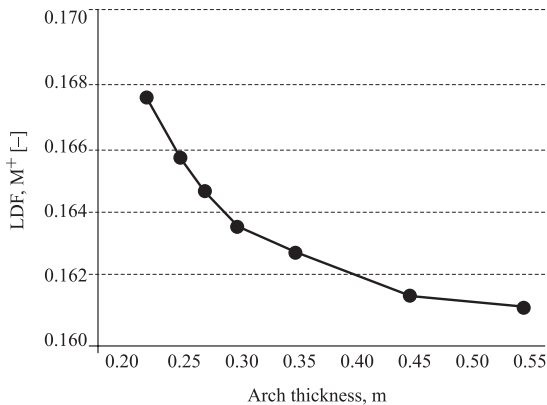
5. Conclusions

1. The full-scale load tests attested the good structural response of the three types of underpasses studied. In fact, the pattern of variation of radial deflections was continuous and agreed with the typical behaviour exhibited by this type of arch structures. Furthermore, the underpasses presented an elastic behaviour with negligible cracking and an almost full recovery of deflections.

2. Numerical results obtained with the 3D FE models developed within the present study were in good agreement with their experimental counterparts, considering the locations and magnitudes of the peak values of vertical displacements. The generally good agreement between experimental and numerical results, particularly if taking into account the non-linearity and randomness of the soil, allowed validating the models developed.

3. The comparison of the effects of design loads defined in *EN 1991-2:2003 Eurocode 1: Actions on Structures – Part 2: Traffic Loads on Bridges* (EC1) and those of the *Portuguese Code for the Safety of Buildings and Bridges* (RSA) pointed out the fact that the former standard is much more conservative. Therefore, for most of the existing precast concrete arch underpasses (which were designed

Effect of the arch thickness (cover soil thickness of 0.60 m)



Effect of the cover soil thickness (arch thickness of 0.20 m)

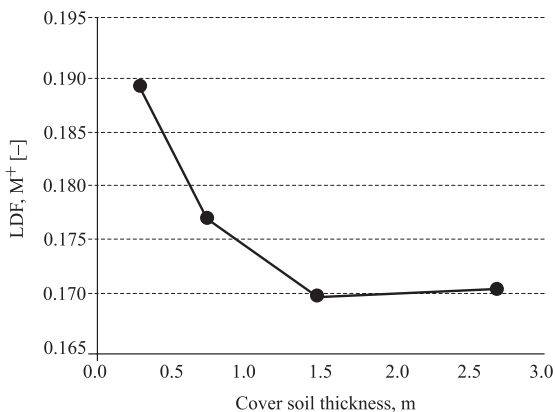


Fig. 9. Load distribution factors in underpass PA2 for M^+

according to RSA), the safety level according to EC1 is insufficient and retrofitting may be needed.

4. The 2D and 3D numerical models developed allowed calculating the load distribution factors (LDFs) for the three underpasses studied, considering different load cases, and the data obtained may be used to design similar precast underpasses.

5. The max LDFs obtained for the three types of underpasses varied between 0.25 and 0.30 (bending), 0.25 and 0.40 (compression), and 0.20 and 0.45 (shear). What concerns bending, LDFs for precast underpasses are considerably lower than those for common deck girders (that vary typically between 0.60 and 0.85), and such difference may be attributed to the cover soil and the additional axial stiffness of the arches.

6. In general, for all types of forces analysed, the variation of LDFs within the three underpasses studied was consistent with their relative stiffness, with the highest values of LDFs corresponding to underpass PA1 (the most flexible) and the lowest to PA3 (the stiffest).

7. As expected, the number of load trucks and their lateral position has a considerable influence in the LDFs. For some cases, when loaded by a single truck, the LDFs corresponding to a lateral position are almost twice than those corresponding to a centred truck. When the number of lateral trucks increases, the LDFs consistently decrease.

8. The parametric study on underpass PA2 showed that, as expected, LDFs for bending moments consistently decrease with the thickness of the arch, approaching a lower bound asymptote of 0.160. The study also showed the consistent reduction of the LDFs with the thickness of the cover soil, with a lower bound of about 0.170 being reached. For design purposes, when using 2D models and for geometries similar to that of underpass PA2, it should be adequate to adopt an LDF of about 0.20.

References

Au, F. T. K.; Wang, J. J.; Liu, G. D. 2003. Construction Control of Reinforced Concrete Arch Bridges, *Journal of Bridge Engineering* 8(1): 39–45.
[http://dx.doi.org/10.1061/\(ASCE\)1084-0702\(2003\)8:1\(39\)](http://dx.doi.org/10.1061/(ASCE)1084-0702(2003)8:1(39)).

- Audenaert, A.; Fanning, P.; Sobczak, L.; Peremans, H. 2008. 2-D Analysis of Arch Bridges Using an Elasto-Plastic Material Model, *Engineering Structures* 30(3): 845–855.
<http://dx.doi.org/10.1016/j.engstruct.2007.05.018>.
- Boothby, T. E.; Domalik, D. E.; Dalal, V. A. 1998. Service Load Response of Masonry Arch Bridges, *Journal of Structural Engineering* 124(1): 17–23.
[http://dx.doi.org/10.1061/\(ASCE\)0733-9445\(1998\)124:1\(17\)](http://dx.doi.org/10.1061/(ASCE)0733-9445(1998)124:1(17)).
- Chen, B. G.; Zheng, J. J.; Han, J. 2010. Experimental Study and Numerical Simulation on Concrete Box Culverts in Trenches, *Journal of Performance of Constructed Facilities* 24(3): 223–234.
[http://dx.doi.org/10.1061/\(ASCE\)CF.1943-5509.0000098](http://dx.doi.org/10.1061/(ASCE)CF.1943-5509.0000098).
- Cusens, A. R.; Pama, R. P. 1975. *Bridge Deck Analysis*. 1st edition. London: John Wiley and Sons, 294 p. ISBN 0471189987.
- Fanning, P. J.; Boothby, T. E.; Roberts, B. J. 2001. Longitudinal and Transverse Effects in Masonry Arch Assessment, *Construction and Building Materials* 15(1): 51–60.
[http://dx.doi.org/10.1016/S0950-0618\(00\)00069-6](http://dx.doi.org/10.1016/S0950-0618(00)00069-6).
- Fanning, P. J.; Boothby, T. E. 2001. Three-Dimensional Modelling and Full-Scale Testing of Stone Arch Bridges, *Computers and Structures* 79(29–30): 2645–62.
[http://dx.doi.org/10.1016/S0045-7949\(01\)00109-2](http://dx.doi.org/10.1016/S0045-7949(01)00109-2).
- Hambly, E. C. 1976. *Bridge Deck Behaviour*. 2nd edition. London: Taylor & Francis, 336 p. ISBN 0419172602.
- Kamaitis, Z. 2012. Influence of Functionally Obsolete Bridges on the Efficiency of Road Network. Part I: Obsolescence Characteristics and Assessment, *The Baltic Journal of Road and Bridge Engineering* 7(3): 173–180.
<http://dx.doi.org/10.3846/bjrbe.2012.24>.
- Pimentel, M.; Costa, P.; Félix, C.; Figueiras, J. 2009. Behavior of Reinforced Concrete Box Culverts under High Embankments, *Journal of Structural Engineering* 135(4): 366–375. [http://dx.doi.org/10.1061/\(ASCE\)0733-9445\(2009\)135:4\(366\)](http://dx.doi.org/10.1061/(ASCE)0733-9445(2009)135:4(366)).
- Zanardo, G.; Pellegrino, C.; Bobisut, C.; Modena, C. 2004. Performance Evaluation of Short Span Reinforced Concrete Arch Bridges, *Journal of Bridge Engineering* 9(5): 424–434.
[http://dx.doi.org/10.1061/\(ASCE\)1084-0702\(2004\)9:5\(424\)](http://dx.doi.org/10.1061/(ASCE)1084-0702(2004)9:5(424)).
- Zoghi, M.; Farhey, D. N. 2006. Performance Assessment of a Precast-Concrete, Buried, Small Arch Bridge, *Journal of Performance of Constructed Facilities* 20(3): 244–252.
[http://dx.doi.org/10.1061/\(ASCE\)0887-3828\(2006\)20:3\(244\)](http://dx.doi.org/10.1061/(ASCE)0887-3828(2006)20:3(244)).

Received 14 February 2011; accepted 5 July 2011